

See discussions, stats, and author profiles for this publication at: <https://www.researchgate.net/publication/231681142>

# Surface and Solid-State Properties of a Fluorinated Polyelectrolyte–Surfactant Complex

ARTICLE *in* LANGMUIR · JUNE 1999

Impact Factor: 4.46 · DOI: 10.1021/la9900728

---

CITATIONS

36

---

READS

17

2 AUTHORS, INCLUDING:



Andreas F Thünemann

Bundesanstalt für Materialforschung und -pr...

178 PUBLICATIONS 4,958 CITATIONS

SEE PROFILE

# Surface and Solid-State Properties of a Fluorinated Polyelectrolyte–Surfactant Complex

Andreas F. Thünemann<sup>\*,†</sup> and Kai Helmut Lochhaas<sup>‡</sup>

Max Planck Institute of Colloids and Interfaces, Am Mühlenberg, 14476 Golm, Germany, and  
Colloid Surface Technologies GmbH, Industriepark Kalle-Albert, Rheingastrasse 190-196,  
65174 Wiesbaden, Germany

Received January 25, 1999. In Final Form: April 7, 1999

The complexation of poly[(acrylamidopropyl)trimethylammonium chloride] with sodium [bis(perfluorohexylethyl)-2-sulfosuccinate] (Fluowet SB) in aqueous solution results in a highly ordered mesomorphous polyelectrolyte–surfactant complex. Films prepared from the complex exhibited a remarkably low critical surface tension of 6 mN/m, which was determined by dynamic contact angle data. Small-angle X-ray scattering data revealed the structure to be lamellar with repeat units in the range 3.48–3.90 nm, depending on the water content. Atomic force microscopy (AFM) allowed the film surface to be visually represented. It consists of characteristic elevations and depressions. The distance between the elevations ranges from 100 to 300 nm, and the elevations have a uniform height of about 3.4 nm, which confirms their lamellar structure. A detailed investigation of the viscoelastic properties was carried out using dynamic mechanical measurements. Master curves of the storage moduli of dry and wet samples were calculated.

## Introduction

The importance of fluorinated polymers results from their unique property of repelling both oil and water. A great deal of development work aimed at enhancing and optimizing these properties has already been conducted. However, the use of fluorinated polymers is still restricted due to their poor solubility, difficulties in formulating coatings, and high costs. From a practical and theoretical point of view it is important that, among various possible molecular structures, the closest-packed uniform CF<sub>3</sub> surface was found to display the lowest surface tension ever measured (6 mN/m),<sup>1</sup> a value which is much lower than that of poly(tetrafluoroethylene) (20 mN/m). There have been several promising attempts to produce surfaces highly enriched with CF<sub>3</sub> groups by the development of self-organizing materials, such as Langmuir–Blodgett monolayers,<sup>2,3</sup> fluorinated block copolymers,<sup>4,5</sup> semifluorinated side-chain ionenes,<sup>6</sup> and fluorinated poly(α,L-glutamate)s.<sup>7</sup> Solid complexes of polyelectrolytes with fluorinated surfactants are a family of materials that exploit self-organization in order to form surfaces highly enriched in CF<sub>3</sub> groups.<sup>8,9</sup> Recently, we reported on a waterborne nanodispersion of a fluorinated complex that can be used as a coating material for smooth surfaces which does not affect the appearance of the surface.<sup>10</sup>

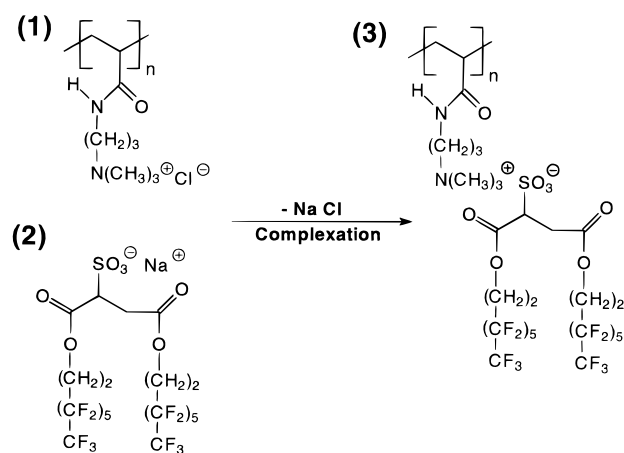


**Figure 1.** Scheme of complex formation: (1) poly[(acrylamidopropyl)trimethylammonium chloride]; (2) sodium [bis(perfluorohexylethyl)-2-sulfosuccinate]; (3) stoichiometric polyelectrolyte surfactant complex.

Further, it was demonstrated that such a self-organizing complex could, in principle, be applied without difficulty in formulating.

The work here reports on the structure and mechanical properties of a new fluorinated surfactant-containing polymer complex which forms ordered colloidal structures and surfaces with an extremely low surface energy. Complex 3 is prepared (Figure 1) by precipitation from aqueous solution using poly[(acrylamidopropyl)trimethylammonium chloride] (1) and sodium [bis(perfluorohexylethyl)-2-sulfosuccinate] (Fluowet SB) (2). The influence of water on the structure and the property behavior has been quantified.

## Experimental Section

**A. Materials.** For complexation we used two commercially available compounds: The first was poly[(acrylamidopropyl)trimethylammonium chloride] produced by Stockhausen GmbH

\* Corresponding author. Telephone: +49-331-567-9544. E-mail: andreas@terra.mpikg-golm.mpg.de.

<sup>†</sup> Max Planck Institute of Colloids and Interfaces.

<sup>‡</sup> Colloid Surface Technologies GmbH.

(1) Schulman, F.; Zisman, W. A.; Hare, E. F.; Shafrin, E. G.; Zisman, W. A. *J. Colloid Sci.* **1954**, *58*, 236.

(2) Schönherr, H.; Ringsdorf, H. *Langmuir* **1996**, *12*, 3891.

(3) Schönherr, H.; Ringsdorf, H.; Jaschke, M.; Butt, H.-J.; Bamberg, E.; Allinson, H.; Evans, S. D. *Langmuir* **1996**, *12*, 3898.

(4) Wang, J.; Mao, G.; Ober, C. K.; Kramer, E. J. *Macromolecules* **1997**, *30*, 1906.

(5) Antonietti, M.; Förster, S.; Micha, M. A.; Oestreich, S. *Acta Polym.* **1997**, *48*, 262.

(6) Wang, J.; Ober, C. K. *Macromolecules* **1997**, *30*, 7560.

(7) Dessipri, E.; Tirrell, D. A.; Atkins, E. D. T. *Macromolecules* **1996**, *29*, 3545.

(8) Antonietti, M.; Henke, S.; Thünemann, A. F. *Adv. Mater.* **1996**, *8*, 41.

(9) Thünemann, A. F.; Lochhaas, K. H. *Langmuir* **1998**, *14*, 4898.

(10) Thünemann, A. F.; Lieske, A.; Paulke, B.-R. *Adv. Mater.* **1999**, *11*, 321.

(Krefeld). The polymer was purified by ultrafiltration (membrane 10 K) and subsequently freeze-dried. The weight- and number-average molecular weights of the polyelectrolyte (**1**) are  $M_w = 66\,000$  g/mol and  $M_n = 38\,000$  g/mol (Figure 1). The molecular weight was determined by gel permeation chromatography (GPC, 0.5 mol/dm<sup>3</sup> NaNO<sub>3</sub>, Progel-TSK-PW column by Tosohaas, refraction index and a light-scattering detector). The second compound was Fluowet SB (Clariant), a fluorinated surfactant, mainly containing sodium [bis(perfluorohexylethyl)-2-sulfosuccinate] (**2**). Fluowet SB is produced from sulfosuccinic acid, esterified with two fluorinated chains. The perfluorinated alkyl chain length distribution is relatively narrow, with about 95% of the side chains containing terminal perfluoro-*n*-hexyl groups. The remaining 5% are a distribution of perfluoro-*n*-octyl, perfluoro-*n*-decyl, and perfluoro-*n*-dodecyl groups. Fluowet SB is commonly used as an active spreading agent.<sup>11</sup> As a solvent for the complex, 2,2,2-trifluoroethanol (Aldrich, 99.5%) was used.

**B. Preparation.** Sodium [bis(perfluorohexylethyl)-2-sulfosuccinate] (20 mmol; 13.4 g) was dissolved in 200 mL of water (Millipore) and stirred at 70 °C. To this, a solution of 1.0 equiv (4.14 g) of polyelectrolyte in 100 mL of water was added in droplets (the stoichiometry was calculated with respect to the charges). A solid polyelectrolyte-surfactant complex was obtained as a white precipitate. The complex (**3**) was isolated, washed three times with 100 mL of 70 °C water, and dried for 24 h at 0.1 mbar. Elemental analysis for the complex obtained [observed (calculated for 1:1 stoichiometry)]: C, 32.0 (32.9); H, 2.9 (2.8); N, 2.8 (2.6); Cl, <0.01 (0). The complex was dissolved in 2,2,2-trifluoroethanol and cast on a glass sheet. The two-dimensional geometry of the films is stabilized by a glass frame, which was mounted on top of the glass sheet, comparable to the procedure described earlier.<sup>27</sup> After the evaporation of the solvent, films could be easily removed and cut. The thicknesses of the films used for measuring bulk properties were in the range 0.1–1 mm. Before investigation they were stored first in a vacuum for 12 h followed by a subsequent storage at 23 °C and 30% relative humidity (dry complex) for 1 week and 100% humidity (wet complex) for 1 week.

**C. Methods.** The thickness of the complex coatings was determined by using a surface profiler Dektak<sup>3</sup>ST from Veeco Instruments. Contact angle measurements were performed on a Krüss G10 contact angle goniometer; the angles reported here are the average of five measurements. The advancing contact angle was read by injecting a 5  $\mu$ L liquid droplet, the receding contact angle was measured by removing about 3  $\mu$ L of liquid from the droplet, and the static contact angle was obtained from a droplet (ca. 5  $\mu$ L) on the surface. Linear alkanes, methyl-terminated poly(dimethylsiloxane) oligomer (Geltest Inc.),  $\alpha$ -bromonaphthalene, diiodomethane, and water (Millipore) were used as test liquids. Wide-angle X-ray scattering (WAXS) measurements were carried out with a Nonius PDS120 powder diffractometer in transmission geometry. A FR590 generator was used as the source of Cu K $\alpha$  radiation, monochromatization of the primary beam was achieved by means of a curved Ge crystal, and the scattered radiation was measured with a Nonius CPS120

position sensitive detector. The resolution of this detector is about 0.018°. Small-angle X-ray scattering measurements were recorded with an X-ray vacuum camera with pinhole collimation (Anton Paar, Austria; model A-8054) equipped with image plates (type BAS III, Fuji, Japan). The image plates were read with a MACScience Dip-Scanner IPR-420 and IP reader DIPR-420 (Japan). Differential scanning calorimetry (DSC) measurements were performed on a Netzsch DSC 200 (Germany). The samples were examined at a scanning rate of 15 K/min by applying one cooling and two heating scans. The glass transition temperatures were determined as midpoints. Thermogravimetric analysis (TGA) was performed in nitrogen atmosphere and with a heating rate of 5 K/min using a Netzsch TG 209 instrument. For determination of the complex shear modulus  $G^* = G' + iG''$ , dynamic mechanical measurements were carried out using a Netzsch DMA 242 in sandwich geometry at the heating rate 1 K/min. The frequencies used were 0.05, 0.1, 0.2, 0.5, 1, 2, 5, and 10 Hz. Atomic force microscopy (AFM) was carried out with a Nanoscope IIIa (Digital Instruments) in tapping mode.

## Results and Discussion

**A. Surface Energies.** Films of complex **3** were prepared by casting a 0.1% (w/w) complex solution on smooth but chemically different surfaces such as glass and aluminum. The coated surfaces were dried, washed extensively with water, and dried again, thus forming thin coatings with thicknesses in the range 300–500 nm. The dynamic contact angles  $\theta$  of the test liquids with different surface tensions were measured by means of the sessile drop method<sup>12</sup> (Table 1). It was found in particular that all nonpolar liquids, which spread readily on uncoated surfaces, showed high contact angles on complex-coated surfaces. However, direct measurement of the surface energies of nonelastomeric solid materials is not simple. For practical reasons, procedures based on contact angle measurements are regularly used.<sup>13–19</sup> Neumann and Li derived an equation of state by which it is possible to calculate the surface free energy:<sup>20</sup>

$$\cos \theta = -1 + 2\sqrt{\frac{\gamma_s}{\gamma_l}} \exp(-\beta(\gamma_l - \gamma_s)^2) \quad (1)$$

where  $\beta$  is a constant (0.000 124 7 m<sup>2</sup> mJ<sup>-1</sup>). Thus, the surface energy  $\gamma_s$  of the solid can be determined from experimental contact angles and the liquid surface tension  $\gamma_l$ . The surface energies calculated using eq 1 range from 7.4 to 10.5 mN/m for all test liquids, with surface tensions in the range 18.4–50.0 mN/m (Table 1). These values are significantly lower than the surface energies found for the fluorinated polymer (FC-725)-coated wafers,<sup>19</sup> which range from 11.8 to 13.2 mN/m. No significant difference was found for the surface energies calculated for complex coated surfaces on glass, aluminum, or silicon wafers. Therefore, it is very probable that the thickness of the complex of about 300–500 nm is large enough to avoid boundary effects caused by the substrate. The coated substrate influences the complex structure most strongly at or near to the complex/air interface. The critical surface tension  $\gamma_c$  of a surface can often be determined from the contact angles of a homologous series of nonpolar liquids.<sup>13</sup>  $\gamma_c$  defines the wettability of a solid by noting the lowest surface tension a liquid can have and still exhibit a contact angle greater than 0°. The  $\gamma_c$  value of a surface is usually obtained from a Zisman plot of the contact angles,<sup>13</sup> such that a plot of  $\cos \theta$  against the surface tensions of liquids  $\gamma_l$  is a straight line with the slope  $m$ :

$$\cos \theta = 1 + m(\gamma_l - \gamma_c) \quad (2)$$

The extrapolation of  $\gamma_l$  to  $\cos \theta = 1$  gives  $\gamma_c$ . Zisman plots

(11) Information supplied by the manufacturer: Hoechst AG, Frankfurt, Germany.

(12) Augsburg, A.; Grundke, K.; Pöschel, K.; Jacobasch, H.-J.; Neumann, A. W. *Acta Polym.* **1998**, *49*, 417.

(13) Zisman, W. A. *Ind. Eng. Chem.* **1963**, *55*, 18.

(14) Fowkes, F. M. *J. Phys. Chem.* **1962**, *66*, 382.

(15) Girifalco, L. A.; Good, R. J. *J. Phys. Chem.* **1957**, *61*, 904.

(16) Drummond, C. J.; Georgaklis, G.; Chan, D. Y. C. *Langmuir* **1996**, *11*, 2617.

(17) Höpken, J.; Möller, M. *Macromolecules* **1992**, *25*, 1461.

(18) Wang, J.; Ober, C. K. *Macromolecules* **1997**, *30*, 7560.

(19) Kwok, D. Y.; Lam, C. N. C.; Li, A.; Leung, A.; Wu, R.; Mok, E.; Neumann, A. W. *Colloids Surf.* **1998**, *142*, 219.

(20) Li, D.; Neumann, A. W. *J. Colloid Interface Sci.* **1992**, *148*, 190.

(21) Hare, E. F.; Shafring, E. G.; Zisman, W. A. *J. Colloid Sci.* **1954**, *58*, 236.

(22) Yasuda, H.; Okuno, T.; Sawa, Y.; Yasuda, T. *Langmuir* **1995**, *11*, 3255.

(23) Neinhuis, C.; Barthlott, W. *Ann. Bot. (London)* **1997**, *79*, 667.

(24) Barthlott, W.; Neinhuis, C. *Planta* **1997**, *202*, 1.

(25) WO 96/04123.

(26) Onda, T.; Shibuichi, S.; Satoh, N.; Tsujii, K. *Langmuir* **1996**, *12*, 2125.

(27) Antonietti, M.; Conrad, J.; Thünemann, A. F. *Macromolecules* **1994**, *27*, 6007.

**Table 1. List of Contact Angles of Different Test Liquids on Materials Coated with Complex 3 at 20 °C**

solvent	$\gamma_1$ (mN/m)	advancing angle (deg) <sup>b</sup>	stationary angle (deg) <sup>b</sup>	receding angle (deg) <sup>b</sup>	$\gamma_s$ (mN/m)
Glass Slide					
hexane	18.4	60	57	41	10.5
PDMS <sup>c</sup>	18.7	62	62	60	10.2
octane	21.8	70	70	63	10.1
decane	23.9	73	72	70	10.4
dodecane	25.4	76	76	70	10.3
hexadecane	27.6	82	80	74	9.7
$\alpha$ -bromonaphthalene	44.0	102	100	92	9.3
methylene iodide	50.0	113	109	100	8.3
water	72.7	82	75	70	34.2
Aluminum Sheet					
hexane	18.4	60	57	41	10.5
PDMS <sup>c</sup>	18.7	62	62	60	10.2
octane	21.8	70	70	63	10.1
decane	23.9	73	72	70	10.4
dodecane	25.4	76	76	70	10.3
hexadecane	27.6	82	80	74	9.7
$\alpha$ -bromonaphthalene	44.0	102	100	92	9.3
methylene iodide	50.0	113	109	100	8.3
water	72.7	82	75	70	34.2

<sup>a</sup> The surface tensions of the test liquids  $\gamma_1$  and advancing, stationary, and receding contact angles measured by a Krüss contact angle goniometer are listed.  $\gamma_s$  is the surface energy calculated by using eq 1 and advancing contact angles. <sup>b</sup> Error of measurement ca. 1°. <sup>c</sup> Commercial product of poly(dimethylsiloxane) oligomers (trimethylsiloxy terminated) from Geltest Inc.

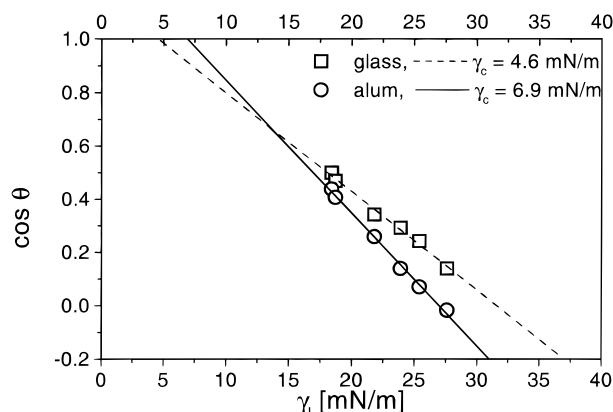


**Figure 2.** Zisman plots for two complex-coated surfaces. Points are obtained with (1) hexane,  $\gamma_1 = 18.4$  mN/m; (2) PDMS,  $\gamma_1 = 18.7$  mN/m; (3) octane,  $\gamma_1 = 21.8$  mN/m; (4) decane,  $\gamma_1 = 23.9$  mN/m; (5) dodecane,  $\gamma_1 = 25.4$  mN/m; and (6) hexadecane,  $\gamma_1 = 27.6$  mN/m. The critical surface tension of a complex on glass was calculated to be  $4.6 \pm 1.4$  mN/m by extrapolating a linear fit (dashed line) of the  $\cos \theta$  (cycles) to  $\cos \theta = 1$ . For aluminum (cycles) a critical surface tension of  $6.9 \pm 0.8$  mN/m was determined (straight line). Advancing contact angles were used for  $\cos \theta$ .

**Table 2. Zisman Critical Surface Energies  $\gamma_c$  and the Dispersive Surface Energies  $\gamma_s^d$  According to the Girifalco–Fowkes–Young Equation of Complex Films on Aluminum and Glass**

substrate	$\gamma_c$ (mN/m)	$\gamma_s^d$ (mN/m)
aluminum	$6.9 \pm 0.8$	$8.1 \pm 0.4$
glass	$4.6 \pm 1.4$	$9.3 \pm 0.5$

result in critical surface tensions of  $6.9 \pm 0.8$  mN/m for aluminum and  $4.6 \pm 1.4$  mN/m for glass as material for coating (Figure 2 and Table 2). Within the experimental range of error, which was measured for an oriented close-packed monolayer of perfluorododecanoic acid, both values are equal to the lowest critical surface tension observed to date (6 mN/m).<sup>21</sup> It is widely accepted that such low critical surface tensions characterize the resulting properties of a surface of closed-packed perfluoromethyl  $\text{CF}_3$  groups.<sup>4,21</sup> Therefore, we conclude that the complex-coated surfaces presented are strongly enriched with  $\text{CF}_3$  groups.

It must be stressed here that although  $\gamma_c$  values are widely used for surface characterization, there is no theoretical justification for equating the critical surface tension with the surface energy of a material. The wettability data were also used to determine the dispersion force component of the surface energy  $\gamma_s^d$  by using the Girifalco–Good–Fowkes–Young equation,<sup>14,15</sup> which has the form

$$\cos \theta = -1 + 2\sqrt{\frac{\gamma_s^d}{\gamma_1}} \quad (3)$$

and has been theoretically justified. This equation is utilized by plotting  $\cos \theta$  against  $(1/\gamma_1)^{1/2}$  for a family of dispersive liquids with the ordinate of the best linear fit located at  $-1$  and the gradient being  $2(\gamma_s^d)^{1/2}$ . The Girifalco–Good–Fowkes–Young plots are used to show the dynamic advancing contact angle data obtained for complex surfaces on glass and aluminum substrates (Figure 3). Linear fits result in dispersive surface energies of  $\gamma_s^d = 8.1 \pm 0.4$  and  $9.3 \pm 0.5$  mN/m for aluminum and glass, respectively (Table 2). These values are close to those found for a highly fluorinated side-chain homopolymer, *p*-[[[(perfluorooctylethylene)oxy]methyl]styrene ( $9.3$  mN/m<sup>17</sup>). Both  $\gamma_c$  and  $\gamma_s^d$  values indicate a rather ordered packing of the perfluorinated segments, exposing  $\text{CF}_3$  groups on the surface. It is particularly interesting that the contact angle of water (the most polar test liquid with  $\gamma_1 = 72.7$  mN/m) is smaller than that of methylene iodide ( $\gamma_1 = 50.0$  mN/m). The calculated surface energy using the equation of state (eq 1) was determined to be  $34.2$  mN/m. The low surface energies determined for nonpolar liquids were reproduced, even when the complex-coated surfaces were dried after reimmersion in water. This indicates a reversible reconstruction of the complex surface after it has been in contact with water. By contrast, the low-energy-surface-forming coatings of perfluorinated acids adsorbed on platinum where removed quickly when they came in contact with water.<sup>21</sup> Surface reconstruction phenomena are widespread in polymer coatings, such as self-organizing semifluorinated side-chain ionenes<sup>18</sup> and even polymers containing only a few polar groups, such as Teflon-PFA.<sup>22</sup> It is worth noting that surface recon-



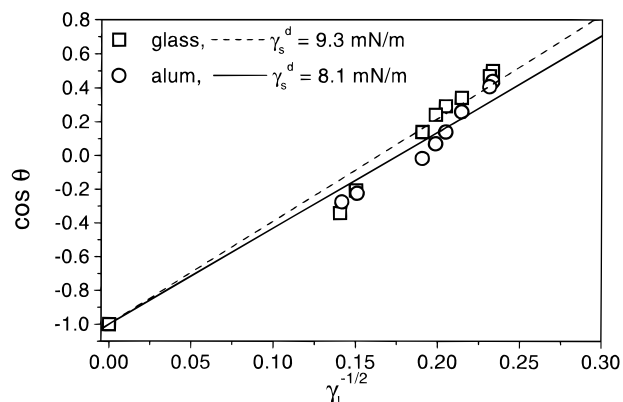


**Figure 3.** Girifalco–Good–Fowkes–Young plots for the determination of the dispersive surface energy of complex-coated surfaces. From left to right the points are values obtained with (1) methylene iodide,  $\gamma_l = 50.0$  mN/m; (2)  $\alpha$ -bromonaphthalene,  $\gamma_l = 44.0$  mN/m; (3) hexadecane,  $\gamma_l = 27.6$  mN/m; (4) dodecane,  $\gamma_l = 25.4$  mN/m; (5) decane,  $\gamma_l = 23.9$  mN/m; (6) octane,  $\gamma_l = 21.8$  mN/m; (7) PDMS,  $\gamma_l = 18.7$  mN/m; and (8) hexane,  $\gamma_l = 18.4$  mN/m. From the slope,  $\gamma_s^d$  was calculated to be  $9.3 \pm 0.5$  mN/m (glass, squares are measured angles, dashed line is least-squares fit) and  $8.1 \pm 0.4$  mN/m (aluminum, cycles are measured angles, solid line is least-squares fit).

structions when in contact with water seem to be very fast, as shown by the constant contact angle of water which adjusts to an equilibrium within some seconds. We suggest that the reason for this could be found on a nanometer scale.

**B. Surface Structure.** Visualization of surfaces of complex **3** films was achieved by AFM. The film surface is smooth even at a micrometer scale, whereas it appears structured on a nanometer scale (Figure 4). This structuring consists of elevations and depressions with the distance between elevations ranging from 100 to 300 nm, resulting in a pattern resembling leopard's fur. Remarkably the elevations have a very uniform height of about 3.4 nm (Figure 5). An important question is whether this surface structuring modifies the surface properties. Indeed, it is well-known that contact angles are influenced by surface roughness. For example, the contact angles of water on the surface of many plant leaves are in the range  $150$ – $170^\circ$ .<sup>23</sup> This high water-repellency originates from micrometer scale surface structures; as a result the name "Lotus flower effect" was coined.<sup>24</sup> The Lotus effect can be mimicked artificial to give antiadhesive surfaces characterized by a structured surface consisting of elevations and depressions, where the distance between the elevations ranges from 5 to  $200 \mu\text{m}$  and the height of the elevations ranges from 5 to  $100 \mu\text{m}$ .<sup>25</sup> The second reason for the observation of extremely high contact angles can be the fractal nature of a surface, as is the case consisting of an alkylketene dimer.<sup>26</sup> Here, the contact angle is given as a function of the fractal dimension, the range of the fractal behavior, and the contacting ratio of the surface. The length scale and roughness morphology observed for complex **3** surfaces cannot be compared to those for a Lotus-like or a fractal surface. According to our knowledge the high values of advancing and static contact angles are not due to the roughness observed on a nanoscale. Nevertheless, this roughness may explain the relatively low receding angles, which are sensitive to physical and chemical heterogeneities. The uniform elevation height of 3.4 nm may be explained by the presence of large islands ( $100$ – $300$  nm) of lamellar complex sheets in a head-to-head double-layer arrangement (Figure 6). Within such islands, the sulfonate head groups are separated by

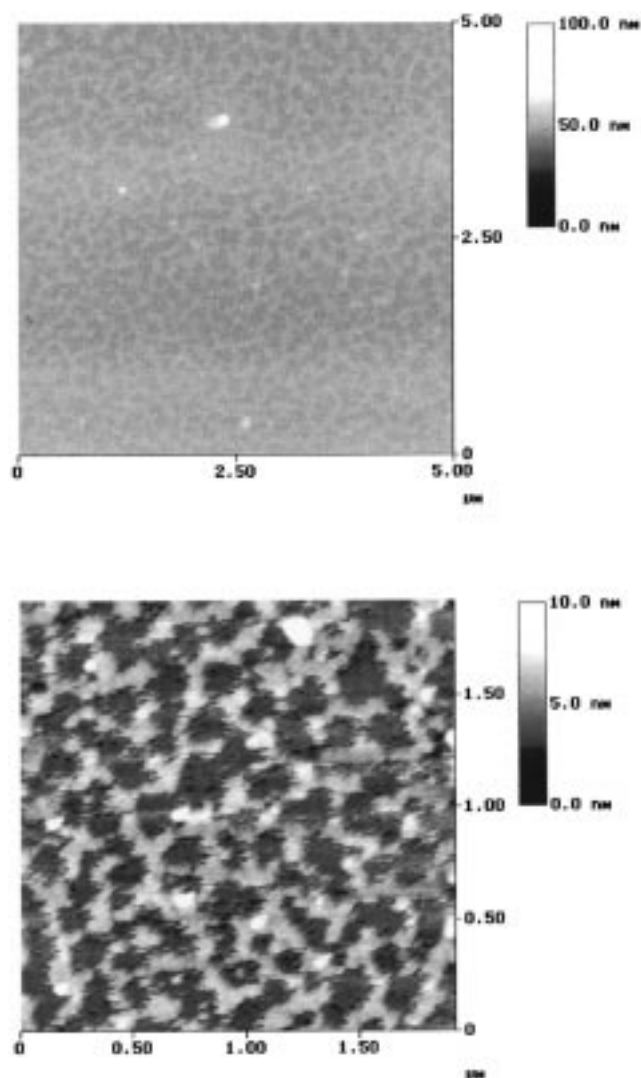


**Figure 4.** AFM image of a complex **3** surface coated on a silicon wafer with different length scales: (a) 5 nm (upper picture); (b) 2 nm (lower picture). Elevations (light) and depressions (dark shaded) are represented. The distance between the elevations ranges from 100 to 300 nm.

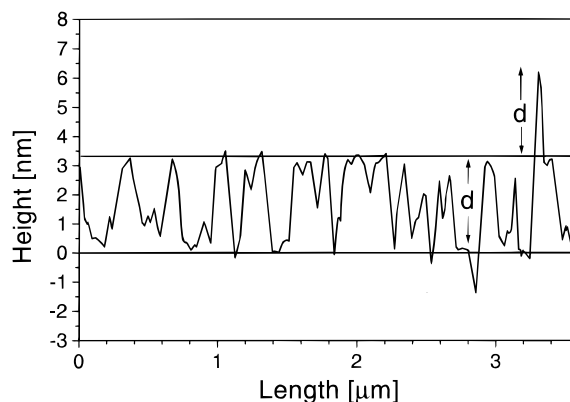


**Figure 5.** Typical AFM depth profile of a complex surface. A uniform height of about 3.4 nm was measured for the elevations, which is originated by a bilayer structure. It can be seen on the right figure that sometimes a second elevation on a first elevation can be found, as would be expected from a bilayer on a bilayer.

cationic polyelectrolyte chains.<sup>27,28</sup> However, the edges of the islands are energetically very unfavorable, allowing highly polar solvent molecules to penetrate into the



**Figure 6.** Sketch of polyelectrolyte–surfactant complex **3** with a lamellar bilayer structure: (a) fluorinated alkyl chains  $\text{CF}_3(\text{CF}_2)_5\text{CH}_2\text{CH}_2$ ; (b) polyelectrolyte chains (not drawn); (c) sulfonate head groups. The repeat unit as found by AFM and SAXS is given as  $d$ .

polyelectrolyte-rich region. Consequently, when in contact with water, a fast surface reorganization occurs, resulting in a much higher-energy surface ( $34.2 \text{ mN/m}$ ) than that observed for nonpolar liquids. This indicates that the thermodynamic equilibrium state of the complex/liquid interface depends on the polarity of the liquid and that water induces a kinetically favored enrichment of polar groups at the edge of the complex islands.

**C. Thermal Analysis.** The incorporation of water modifies not only the surface properties but also the bulk properties of the complex. The thermal stability of **3**, containing different amounts of water, was monitored using TGA. Below  $250^\circ\text{C}$  no significant mass reduction was observed for the water-free complex (Figure 7, solid line), whereas the wet complex displayed a significant weight loss below  $200^\circ\text{C}$  (Figure 7, dashed line), the later being attributed to evaporation of 18% (w/w) water. For both complexes, a weight loss down to about 10% with respect to their dry mass was found in the range from 280 to  $340^\circ\text{C}$ . A final stage of weight loss down to 0% followed in the temperature range from 600 to  $650^\circ\text{C}$ . The striking similarities of both thermograms above  $200^\circ\text{C}$  are interpreted as an identical decomposition of dry and wet complexes. Differential scanning calorimetry (DSC) measurements provided temperature dependent heat capacities of a water-free and a water-containing complex. The water-free complex produced a glass transition temperature ( $T_g$ ) of  $78^\circ\text{C}$  (Figure 8, curve a), whereas the water-containing complex (18% w/w) produced a  $T_g$  of  $36^\circ\text{C}$  (Figure 8, curve b). As expected, drying the water-containing complex prior to DSC measurement produced

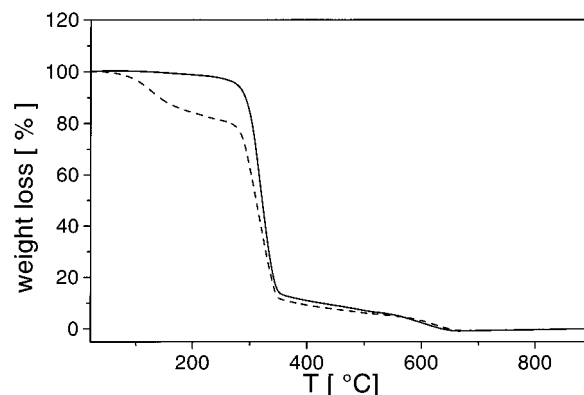


**Figure 7.** Thermogram of complex **3** of a dry (solid line) and wet film (dashed line). The stage below  $200^\circ\text{C}$  in the dashed line was attributed to a water content of 18%.

a  $T_g$  of  $78^\circ\text{C}$ . The position of the glass transition shows that water, which can be easily added and removed, is reversible and acts as a very effective plasticizer for the complex.

**D. Viscoelastic Properties.** The marked dependence of the glass transition temperature on the water content reflects the mechanical properties of the complex. Quantification was achieved using dynamic mechanical measurements of temperature and at different frequencies in the range 0.05–50 Hz. The storage modulus  $G'$ , the loss modulus  $G''$ , and the loss factor  $\tan \delta$  have a similar dependency on temperature and frequency to that typically observed in viscoelastic materials as noncrystalline linear polymers such as polymethacrylates.<sup>29</sup> Isochronal measurements of  $G'$  and  $\tan \delta$  of water-free and water-containing (18% w/w) complexes at frequencies of 0.1, 1,

(28) Micha, M. A.; Burger, C.; Antonietti, M. *Macromolecules* **1998**, *31*, 5930.

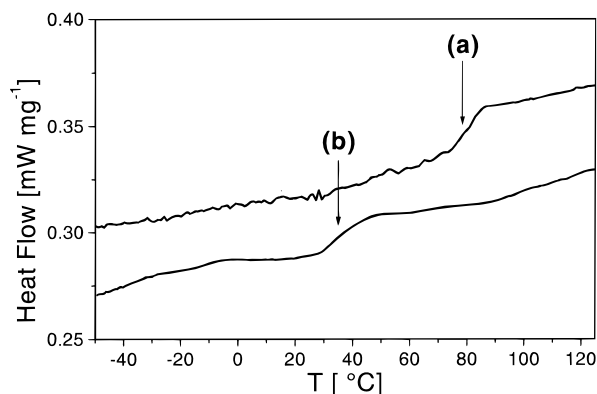


**Figure 8.** DSC heating traces of **3** containing different amounts of water. In the curve of a dry complex, a glass transition temperature was found at 78 °C (a). Due to incorporation of 18% (w/w) water, the glass transition was lowered by 42 °C down to 36 °C (b).

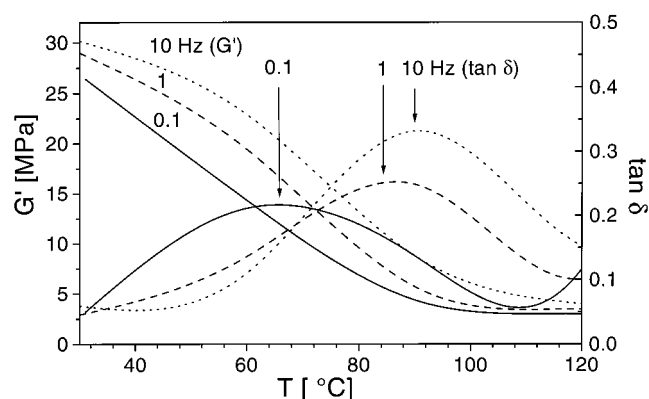


**Figure 9.** Plots of storage modulus and loss tangent against temperature at frequencies of 0.1 Hz (solid line), 1 Hz (dashed line), and 10 Hz (dotted line) for a water-free complex **3**.

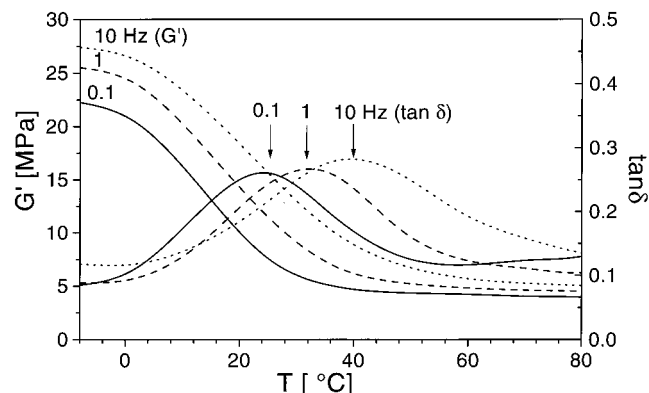


**Figure 10.** Plots of storage modulus and loss tangent against temperature at frequencies of 0.1 Hz (solid line), 1 Hz (dashed line), and 10 Hz (dotted line) for a complex **3** containing 18% water.

and 10 Hz were performed (Figures 9 and Figure 10 respectively). At a given temperature,  $G'$  of the water-free complex increases slightly with increasing frequency, from 26.5 MPa at  $10^{-1}$  Hz to 30.2 MPa at 10 Hz. These values are typical for soft polymers and for rubbers. The water-containing complex at 30 °C has a modulus of 6.0 MPa at  $10^{-1}$  Hz and 13.0 MPa at 10 Hz, a factor of 3 to 4 lower than that of the water-free complex. In the region of the glass transition,  $G'$  decreases sharply, and  $\tan \delta$  as well as  $G''$  has a maximum. For a more extensive comparison of water-free and water-containing complexes, three quantities have been selected as indicators of the

location of the transition zone. These are the frequency where  $G' = 10$  MPa ( $G'_{10}$ ), a value intermediate between those characteristic of the rubber-like and glasslike states,<sup>29</sup> and the temperatures where  $\tan \delta$  and  $G''$  have maxima ( $\tan \delta_{\max}$  and  $G''_{\max}$ ) (Table 3). For the water-free complex  $\tan \delta_{\max}$  shifts from 65 °C ( $10^{-1}$  Hz) to 91 °C (10 Hz), while  $\tan \delta_{\max}$  of the water-containing complex shifts from 24 °C ( $10^{-1}$  Hz) to 39 °C (10 Hz). This shift of  $\tan \delta$  to higher temperatures is accompanied by minor changes in the height of the maximum and the peak widths. The maximum value  $\tan \delta_{\max}$  varies from 0.217 to 0.333. The difference between the water-free complex and the water-containing complex is very small, indicating that the ratio of the loss modulus to the storage modulus at the glass transition temperature is independent of the water content. For all amorphous polymers, whether cross-linked or not, values of  $\tan \delta_{\max}$  in the glass transition zone are in the neighborhood of 1, ranging from 0.2 to 3.<sup>29</sup> The  $\tan \delta_{\max}$  values found for this complex are on the lower limit of this range, thus showing that the complex has a relative high elasticity at  $T_g$ . The maximum values of the loss modulus  $G''_{\max}$  also shift to higher temperatures, but they are located several Kelvin lower than  $\tan \delta_{\max}$ .  $G''_{\max}$  of the water-free complex ranges from 58 °C ( $10^{-1}$  Hz) to 83 °C (10 Hz), and  $G''_{\max}$  of the water-containing complex ranges from 24 °C ( $10^{-1}$  Hz) to 39 °C (10 Hz). To compare the glass-transition temperature found by DSC with the glass transition region determined by dynamic mechanical data,  $\tan \delta_{\max}$  or  $G''_{\max}$  at 1 Hz is often defined as the glass transition temperature. Thus  $T_{g,\tan \delta} = 87$  °C and 33 °C and  $T_{g,G''} = 61$  °C and 21 °C for the water-free and water-containing complex, respectively. Taking  $G' = 10$  MPa, the glass transition locations were found to lie at  $T_{g,G'=10\text{MPa}} = 79$  and 28 °C. The latter shows the best correspondence with the glass transition temperatures determined by DSC (78 and 36 °C). It was found that  $T_g$  for the water-free complex is 40–50 K higher than that of the water-containing complex. This was done independently of the method for determining the glass transition temperature. Master curves for the storage modulus (Figure 11), using the temperature–frequency superposition principle, make it possible to estimate the viscoelastic properties of the complex. Superposition was carried out using Netzsch DMA software, taking 30 °C as the reference temperature. The resulting master curves make estimates of  $G'$  over more than 10 decades possible (Figure 11). On a frequency scale, the shapes of the curves of the water-free and water-containing complexes are rather similar, but the water-containing complex is shifted about 4 to 5 decades to a higher frequency. The functionality of the frequency shift factor  $a_T$  is given by the Williams, Landel, and Ferry (WLF) equation:

$$a_T = - \frac{C_1(T - T_0)}{C_2 + (T - T_0)} \quad (4)$$

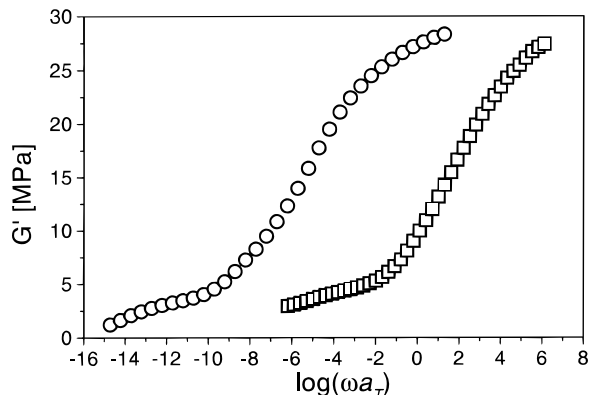
where  $C_1$  and  $C_2$  are temperature-independent constants. The WLF parameters for the water-free complex were calculated to be  $C_1 = 12.2$ ,  $C_2 = 36.0$  K, and  $T_0 = 303$  K; the corresponding values for the water-containing complex were  $C_1 = 14.9$ ,  $C_2 = 98.7$  K, and  $T_0 = 303$  K. These parameters are typical for polymers used widely in daily life, such as polystyrene ( $C_1 = 12.7$ ,  $C_2 = 49.8$  K, and  $T_0 = 373$  K) and poly(methyl acrylate) ( $C_1 = 8.86$ ,  $C_2 = 101.6$  K, and  $T_0 = 324$  K).<sup>29</sup> From the similarity of the viscoelastic properties of polyelectrolyte–surfactant complexes and

(29) Ferry, J. D. In *Viscoelastic Properties of Polymers*, 3rd ed.; Wiley: New York, 1980.



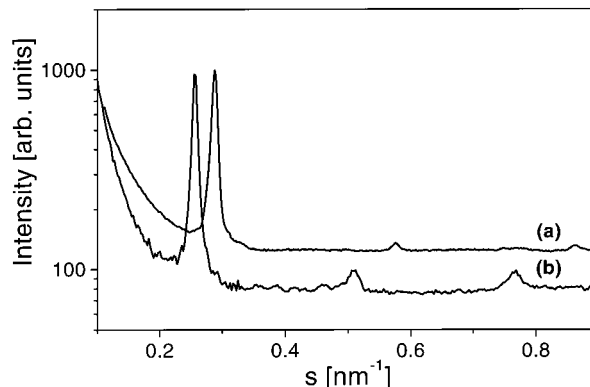
**Table 3. Viscoelastic Parameters of Complex 3 Determined by Dynamic Mechanical Measurements**

water content (% (w/w))	frequency (Hz)	maximum $\tan \delta$ ( $^{\circ}\text{C}$ ), ( )	maximum $G'$ ( $^{\circ}\text{C}$ ), (MPa)	temp at which $G' = 10^7$ Pa ( $^{\circ}\text{C}$ )	$G'$ at 30 $^{\circ}\text{C}$ (MPa)
0	$10^{-1}$	65, 0.217	58, 3.0	71	26.5
0	1	87, 0.260	61, 2.6	79	29.0
0	10	91, 0.333	83, 3.1	87	30.2
18	$10^{-1}$	24, 0.266	13, 2.9	20	6.0
18	1	33, 0.266	21, 2.9	28	9.1
18	10	39, 0.282	24, 3.4	37	13.0

**Figure 11.** Master curves of the storage modulus reduced to 30  $^{\circ}\text{C}$  for a water-free complex (cycles) and a complex containing 18% water (squares).

conventional polymers, it seemed to be very probable that theories developed to describe the mechanical properties of the latter can also be applied to polyelectrolyte–surfactant complexes. The influence of water on the viscoelastic properties has been summarized as that of an effective plasticizer (cf. Sears and Darby: water is the most ubiquitous plasticizer on earth<sup>30</sup>). At the molecular level, water acts as a diluent which enhances the free volume of the complex. In addition, as water enters the ionic-rich region of nonfluorinated complexes,<sup>31</sup> it thus reduces their ionic binding strength. The reduction of the glass transition temperature due to the moisture of the surrounds can be observed for polymers used in daily life. For example, within polyamide structures, water reduces the strength of the hydrogen bonds and the glass transition temperature of Nylon 6 is 76  $^{\circ}\text{C}$  in the dry state and  $-22$   $^{\circ}\text{C}$  at 100% relative humidity at room temperature.<sup>32</sup> Taguchi et al. reported on the viscoelastic properties of films formed by complexes of polystyrenesulfonate and ammonium surfactants.<sup>33</sup> DMA measurements demonstrated that the glass transition can be decreased by shortening the chain length of the surfactant.

**E. X-ray Scattering.** Earlier investigations of polyelectrolyte–surfactant complexes revealed highly ordered mesomorphous structures.<sup>8–10</sup> Similarly, complex **3** was investigated by small- and wide-angle X-ray scattering measurements (Figure 12). Three reflections at equidistant positions are present in the small-angle region, providing additional evidence for the proposed lamellar structure of **3** (Figure 6). In contrast to AFM, the small-angle scattering technique averages over the bulk structure of the complex, thus providing a global “picture”. For

**Figure 12.** X-ray scattering curves of complex **3** ( $s = 2/\lambda \sin \theta$ ,  $\theta$  is the angle between the incident and scattered radiation). The scattering patterns indicate lamellar mesomorphic smectic A-like structures: (a) dry complex with a repeat unit of 3.48 nm; (b) complex containing 18% water with a 12% larger repeat unit of 3.90 nm.

the water-free complex, a lamellar repeat unit of  $d = 3.48$  nm was determined (Figure 12, curve a), which is consistent with the value of 3.4 nm determined by atomic force microscopy. In the small-angle scattering curve of the water-containing complex, the reflex positions are shifted to smaller scattering vectors. This provides evidence for a spreading of the system, thus resulting in a repeat unit of 3.90 nm (Figure 12, curve b). Thus, the repeat unit of the water-containing complex is 0.42 nm (12%) larger than that of the water-free complex. Allowing for experimental error, this is consistent with a homogeneous incorporation of 18% (w/w) water into the ionic layer structure, resulting in a one-dimensional extension of the layer distance. The wide-angle X-ray diagrams displayed only a broad reflection with a  $d$ -spacing of 0.49–0.51 nm which occurred because of the intersegment spacing of the fluorinated chains. This proves that no crystallinity is present in the complex, neither side-chain crystallinity nor crystalline impurities such as sodium chloride.

## Summary and Conclusion

It has been shown that the complexation of a polyelectrolyte (**1**) with a fluorinated surfactant (**2**) results in a lamellar mesomorphous complex (**3**). This complex forms films on different substrates each with very low surface energies. Critical surface tensions are found to be as low as 6 mN/m, which are equivalent to the lowest values observed to date. The complex is insoluble in water; however, when in contact with water, the complex displays a dramatic surface reconstruction, resulting in surface energies of 34.2 mN/m. It is significant that this surface reconstruction is reversible upon redrying. A possible reason for its ability to reconstruct is the leopard-fur-like structuring of the surface which consists of elevations and depression. The height difference of 3.4 nm between elevations and depressions corresponds to the spacing of one double layer, which is identical to the repeat unit

(30) Sears, J. K.; Darby, J. R. *The Technology of Plasticizers*; Wiley: New York, 1982.

(31) Antonietti, M.; Radloff, D.; Wiesner, U.; Spiess, H. W. *Macromol. Chem. Phys.* **1996**, *197*, 2713.

(32) Okajima, K.; Yamane, C.; Ise, F. In *Polymeric Materials Encyclopedia*; Salmone, J. C., Ed.; CRC Press: New York, 1996; Volume 7, p 5391.

(33) Taguchi, K.; Yano, S.; Hiratani, K.; Minoura, N.; Okahata, Y. *Macromolecules* **1988**, *21*, 3328.



determined by small-angle X-ray scattering. The complex incorporates about 18% (w/w) water, when in contact with it, which enlarges the lamellar repeat unit by about 12%. Water acts as a plasticizer by shifting the glass transition temperature 40 to 50 K to lower temperatures. The dynamic mechanical behavior reveals many viscoelastic properties similar to those of typical linear polymers.

**Acknowledgment.** The authors thank Stockhausen GmbH for providing the polyelectrolyte, S. Herminghaus for performing the AFM measurements, H. Löwen for a helpful discussion, and the Max-Planck Society for their financial support.

LA9900728